Miniband structures and densities of impurity states in lateral-surface-superlattice quantum well wires

1994 J. Phys.: Condens. Matter 6 5681

(http://iopscience.iop.org/0953-8984/6/29/010)

J. Phys.: Condens. Matter 6 (1994) 5681–5688. Printed in the UK

Miniband structures and densities of impurity states in lateral-surface-superlattice quantum well wires

Zhen-Yan Deng†‡, Ting-Rong Lai‡, Jing-Kun Guo‡, Hong Sun§ and Shi-Wei Gu§

† Chinese Centre of Advanced Science and Technology (World Laboratory), PO Box 8730, Beijing 100080, People's Republic of China

‡ The State Key Laboratory of High Performance Ceramics and Superfine Microstructure, Shanghai Institute of Ceramics, Chinese Academy of Sciences, Shanghai 200050, People's Republic of China

§ Department of Applied Physics and Institute of Condensed Matter Physics, Shanghai Jiao Tong University, Shanghai 200030, People's Republic of China

Received 6 January 1994, in final form 21 March 1994

Abstract. We calculate energy miniband structures and densities of impurity states in quasi-one-dimensional GaAs/AlAs quantum well wires with periodic lateral surface structures. By a coordinate transformation, the structured interfaces of the wires are transformed into planar interfaces so that the boundary conditions of the electronic wavefunctions can be satisfied exactly on the interfaces. The new optical transition spectral structures associated with minibands and impurities are discussed.

1. Introduction

With the advances in the art of microfabrication, it has become possible to confine the carriers in one, two or all three dimensions (quantum wells, quantum well wires and quantum dots). These structures enable many new phenomena to be discovered and provide potential device applications in future laser technology [1–3] and the optical modulation technique [4]. The presence of impurities in these structures contributes to additional responses when external probes are applied to these systems. Because of the quantum confinement in two directions, the binding energies of impurity states are greatly enhanced in wires compared with those in quasi-two-dimensional quantum well structures [5–18] and the optical absorption spectra associated with impurities in quantum wires are more complicated and interesting than those in quantum wells [19–22].

Recently, a new quantum well structure emerged, in which there are periodic lateral surface structures on its interfaces which act as periodic potentials on an electron. This novel system, referred to as a lateral surface superlattice (LSSL), has shown interesting electronic and optical properties [23–29]. Technically now we are also able to fabricate quantum well wires with periodic structures on their interfaces, referred to as lateral surface superlattice wires (LSSLWs), by ion beam implantation on LSSLs produced by deposition of AlAs and GaAs fractional layers on vicinal GaAs(001) substrates [26, 30], for instance. It is expected that the peculiar electronic and optical properties observed in LSSLs may be greatly enhanced in LSSLWs.

Using the coordinate transformation suggested first by Sun [31], we have studied the electron and impurity states in LSSLWs in our previous papers [32–34]. The results have

0953-8984/94/295681+08$19.50

shown that energy minigaps (EMGs) appear in the electronic energy dispersions in LSSLWs at the boundary of the Brillouin zone, owing to the existence of periodic structured interfaces. The results also showed that the impurity binding energies change along the quantum well wire. In this paper, we study the energy miniband structures and the densities of impurity states in the LSSLW further. The new optical transition spectral structures associated with minibands and impurities in LSSLW will be discussed.

In [11], Bryant has demonstrated that the binding energies for impurities in wires with comparable shapes are most closely correlated to the cross-sectional area and the shape effects on binding energies are of little importance. In this paper, only the LSSLW with a circular cross section is considered to simplify our calculation.

In section 2, we introduce the coordinate transformation and define the effective Hamiltonians. In section 3, the miniband structures in a LSSLW are studied. In section 4, the densities of impurity states in a LSSLW are calculated. A discussion is presented in section 5.

2. The effective Hamiltonians

Let us consider a LSSLW of GaAs surrounded by AlAs, which is assumed to have a circular cross section and an infinitely high potential barrier between GaAs and AlAs. In the effective-mass approximation, the Hamiltonian describing the motion of an electron in the LSSLW can be written as

$$H^{(0)}(r) = \frac{|P^2|}{2m} + V(r) \tag{1}$$

where P and r are the electron momentum and coordinate respectively, and m is the electron-band effective mass. The electron-confining potential well $V(r)$ in the LSSLW is given by

$$V(r) = \begin{cases} 0 & \rho < R_0 + f(r) \\ \infty & \text{elsewhere} \end{cases} \tag{2}$$

where R_0 is the average radius of the LSSLW and $f(r)$ describes the periodic structures on its interfaces.

When a hydrogenic donor impurity is placed in the LSSLW, the Hamiltonian becomes

$$H(r) = \frac{|P^2|}{2m} - \frac{e^2}{\kappa|r - r_i|} + V(r) \tag{3}$$

where $\kappa = 13.1$ is the dielectric constant of GaAs and r_i is the position of the impurity in the LSSLW.

As in [32–34], the following coordinate transformation transforms the structured interfaces of the LSSLW into flat interfaces:

$$\rho' = \rho \frac{R_0}{R_0 + f(r)} \qquad \theta' = \theta \qquad z' = z. \tag{4}$$

In the transformation, we note that

$$\int_V \psi^*(r) H^{(0)}(r) \psi(r)\, d\tau = \int_{V'} \tilde{\psi}^*(r') J(r') \tilde{H}^{(0)}(r') \tilde{\psi}(r')\, d\tau'$$

$$= \int_{V'} \tilde{\psi}^*(r') H^{(0)}_{\text{eff}}(r') \tilde{\psi}(r')\, d\tau' \tag{5}$$

where $J(r')$ is the Jacobian determinant, and the effective Hamiltonians without and with an impurity are defined, respectively, as

$$H_{\text{eff}}^{(0)}(r') = J(r')\tilde{H}^{(0)}(r') \tag{6}$$

$$H_{\text{eff}}(r') = J(r')\tilde{H}(r'). \tag{7}$$

The normalization condition becomes

$$\int_{V'} \tilde{\psi}^*(r')\tilde{\psi}(r')J(r')\,\mathrm{d}\tau' = 1. \tag{8}$$

After the coordinate transformation, the electron-confining potential well $\tilde{V}(r')$ is

$$\tilde{V}(r') = \begin{cases} 0 & \rho' < R_0 \\ \infty & \text{elsewhere.} \end{cases} \tag{9}$$

In the new coordinate system the wavefunction satisfies the boundary condition

$$\tilde{\psi}(r')\,|_{\rho'=R_0} = 0. \tag{10}$$

In this paper, we consider the first type of LSSLW studied in our previous papers [32–34], in which its central line stays straight but the radius of circular cross section fluctuates periodically along the quantum wire. The interface fluctuation is taken as

$$f(r) = \Delta \sin\left(\frac{2\pi}{L_d}z\right) \tag{11}$$

where Δ and L_d are the amplitude and period, respectively, of interface structures.

3. The miniband structures

The electron motion in quantum wires consist of plane waves in the direction along the wires. The periodic structures on the interfaces of the LSSLW act as periodic potentials which cause reflections of the electron plane waves. EMGs appear in the electronic energy dispersions of the LSSLW at the boundary of the Brillouin zone. Now, we calculate the miniband dispersions of the LSSLW with the variational approach:

$$\begin{aligned} E &= \left(\int_V \psi^*(r)H^{(0)}(r)\psi(r)\,\mathrm{d}\tau\right) \Big/ \left(\int_V \psi^*(r)\psi(r)\,\mathrm{d}\tau\right) \\ &= \left(\int_{V'} \tilde{\psi}^*(r')H_{\text{eff}}^{(0)}(r')\tilde{\psi}(r')\,\mathrm{d}\tau'\right) \Big/ \int_{V'} \tilde{\psi}^*(r')\tilde{\psi}(r')J(r')\,\mathrm{d}\tau' \end{aligned} \tag{12}$$

where $\tilde{\psi}(r')$ represents the variational wavefunction in the new coordinate spaces.

When the period of the interface structures of the LSSLW is sufficiently large, we use a very simple two-wave approximation [31] to calculate the first and second miniband dispersions in the LSSLW. That is, the following trial wavefunction is adopted:

$$\tilde{\psi}_{k_z}(r') = A\varphi_{k_z}^{(1)}(r') + B\varphi_{k_z}^{(2)}(r') \tag{13}$$

with

$$\varphi_{k_z}^{(1)}(r') = (\pi R_0^2 L_0)^{-1/2}[J_1(\beta_{01})]^{-1} J_0(\beta_{01}\rho'/R_0)\exp(\mathrm{i}k_z z') \tag{14}$$

$$\varphi_{k_z}^{(2)}(r') = (\pi R_0^2 L_0)^{-1/2}[J_1(\beta_{01})]^{-1} J_0(\beta_{01}\rho'/R_0)\exp[\mathrm{i}(k_z - k_d)z'] \tag{15}$$

where β_{01} is the first zero of the Bessel function, A and B are the variational parameters, $L_0 = NL_d$ ($N \to \infty$) is the length of the LSSLW and $k_d = 2\pi/L_d$ is the first reciprocal-lattice vector. Here, the variational wavefunction (13) satisfies the boundary condition (10). If we insert the trial wavefunction (13) and the effective Hamiltonian (6) into equation (12), the first and second electronic miniband dispersions $E_{1,2}(k_z)$ can be obtained by minimizing E (equation (12)) with respect to A and B, which gives the following equation:

$$\det \| H_{\text{eff}}^{(0)(ij)}(k_z) - E_{1,2}(k_z) J^{(ij)}(k_z) \| = 0 \qquad (i, j = 1, 2) \tag{16}$$

with the matrix elements

$$H_{\text{eff}}^{(0)(ij)}(k_z) = \langle \varphi_{k_z}^{(i)}(r') | H_{\text{eff}}^{(0)}(r') | \varphi_{k_z}^{(j)}(r') \rangle \tag{17}$$

$$J^{(ij)}(k_z) = \langle \varphi_{k_z}^{(i)}(r') | J(r') | \varphi_{k_z}^{(j)}(r') \rangle. \tag{18}$$

After the calculation of equation (16), the first two miniband dispersions $E_{1,2}(k_z)$ are obtained analytically, and their numerical results are given in figure 1 (solid lines).

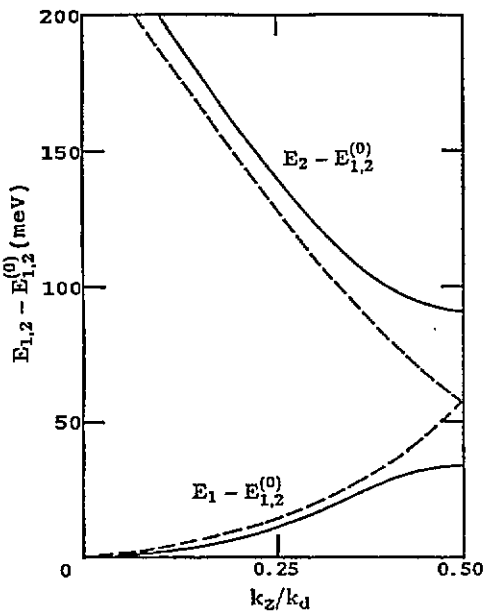

Figure 1. The electronic energy dispersions of the first two conduction minibands $E_{1,2} - E_{1,2}^{(0)}$ with $E_{1,2}^{(0)} = (\hbar^2/2m)(\beta_{01}^2/R_0^2)$ in the LSSLW, where the average radius R_0 of the LSSLW is 50 Å, and the amplitude Δ and period L_d of the interface structures of LSSLW are 10 Å and 100 Å, respectively. The dashed lines represent the corresponding results in the quantum wire without lateral surface structures.

Then we calculate the distribution of the density of electronic states in the first two conduction minibands. The density of electronic states is defined as

$$g(E_{1,2}) = \frac{L_d}{2\pi} \left| \frac{dE_{1,2}}{dk_z} \right|^{-1}. \tag{19}$$

These can be calculated numerically.

The first EMG at the boundary of the Brillouin zone is obtained as

$$\Delta E_g(1) = \frac{\hbar^2}{2m} \frac{\beta_{01}^2}{R_0^2} 2\delta \tag{20}$$

where $\delta = \Delta/R_0$ is the relative fluctuation of the LSSLW in the radial direction.

4. The densities of impurity states

As in our previous papers [33, 34], the electronic wavefunction for the ground state in the new coordinate spaces is taken as

$$\tilde{\phi}_{01}(r') = N_0 J_0(\beta_{01}\rho'/R_0) \tag{21}$$

where N_0 is the normalization constant. Here, the periodic potential due to the periodic interface structures is much smaller than the electronic kinetic energy, and the electronic wavefunction moving along the LSSLW could be viewed as a plane wave.

The trial wavefunction that we take for the effective Hamiltonian $H_{\text{eff}}(r')$ with an impurity is analogous to that used in [10, 14] and is written for the ground impurity state as

$$\tilde{\psi}(r') = N J_0(\beta_{01}\rho'/R_0)\exp(-|r' - r_i'|/\lambda) \tag{22}$$

where N is the normalization constant and λ is the variational parameter.

As usual, we define the impurity binding energy as the energy difference between the bottom of the electronic conduction band without the impurity and the ground-state energy level of an impurity state in the LSSLW, i.e.

$$E_i = \langle\tilde{\phi}_{01}(r')|H_{\text{eff}}^{(0)}(r')|\tilde{\phi}_{01}(r')\rangle - \min_{\lambda}\langle\tilde{\psi}(r')|H_{\text{eff}}(r')|\tilde{\psi}(r')\rangle. \tag{23}$$

According to the geometric symmetry of the LSSLW, we calculate the impurity binding energies only in half the lateral period, i.e. $\frac{1}{2}L_d$, in the z direction in the LSSLW.

Assuming that the circular cross section of the LSSLW is not too small, we could treat the impurity position as a continuous random variable. Provided that the impurities exist only inside the LSSLW and there is no intentional doping, in the new coordinate spaces, one can define a density of impurity states per unit binding energy as

$$g(E_i) = \frac{1}{V_0}\int_{s(E_i)} \frac{ds'}{|\nabla_{r_i'} E_i(r_i')|} \tag{24}$$

where V_0 is the volume of the LSSLW in half the lateral period, i.e. $\frac{1}{2}L_d$, $s(E_i)$ is the portion of the area $E_i = E$ lying within half the lateral period in LSSLW and $\nabla_{r_i'}$ means the gradient with respect to the impurity position. When the relative fluctuation in the radial direction is small and the lateral period L_d is sufficiently large, by neglecting the second- and high-order perturbations proportional to δ the density of impurity states could be further simplified as

$$g(E_i) = \frac{2}{L_d}\int_{-L_d/4}^{L_d/4} g_0(E_i, z_i')\,dz_i' \tag{25}$$

with

$$g_0(E_i, z_i') = \frac{1}{S_0}\int_{L(E_i)} \frac{dL'}{|\nabla_{\rho_i'} E_i(\rho_i', z_i')|} = \frac{2}{R_0^2}\rho_i'\left|\frac{dE_i}{d\rho_i'}\right|^{-1} \tag{26}$$

which is the analogue of the density of impurity states in a cylindrical quantum well wire without lateral surface structures [16], where $L(E_i)$ is the portion of the line $E_i = E$ lying within the circular cross section at $z' = z_i'$, S_0 is the area of circular cross section and $\nabla_{\rho_i'}$ represents the gradient with respect to the impurity position within the cross section at $z' = z_i'$.

Figure 2 shows the density of donor impurity states as a function of binding energy in the LSSLW (solid line). From figure 2, it can be easily seen that a tail structure in the density of impurity states of the LSSLW emerges compared with that of quantum well wire without lateral surface structures (dashed line), and the impurity binding energy in the LSSLW extends on the maximum and minimum binding energy sides.

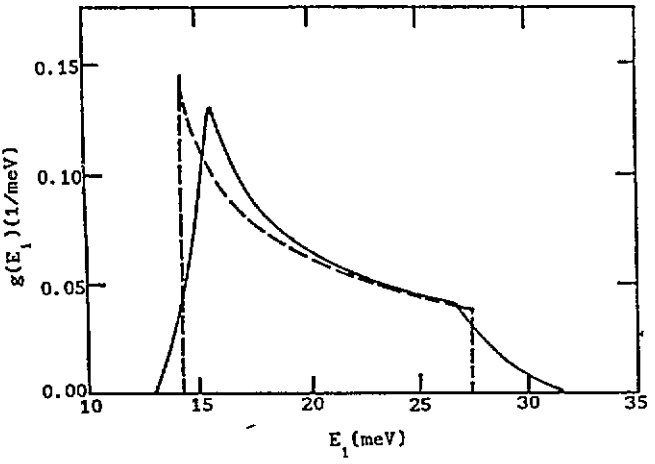

Figure 2. The density of donor impurity states as a function of binding energy in the LSSLW, where the average radius R_0 of LSSLW is 50 Å, and the amplitude Δ and the period L_d of the interface structures of the LSSLW are 10 Å and 100 Å, respectively. The dashed line represents the density of impurity states in the quantum wire without lateral surface structures.

5. Discussion

In this paper, we calculate the energy miniband structures and the densities of impurity states in the LSSLW. The electronic states in the LSSLW differ considerably from those in quantum well wires with planar interface structures, owing to the periodic potential perturbation along the LSSLW direction caused by the periodic surface structures. From figure 1, it is shown that the electronic continuous conduction band spectrum breaks into minibands with minigaps appearing at the edge of the Brillouin zone in the reciprocal-vector space. The change in the electronic states is also reflected in the change in the electronic density of states of the LSSLW, as shown in figure 3(*a*). New peaks and gaps appear in the electronic density of states at the energies near the edge of the Brillouin zone. The first minigap of the conduction minibands is $\Delta E_g^c(1) = 52.6$ meV if we assume that the average radius R_0 of the GaAs/AlAs LSSLW equals 50 Å and the amplitude Δ of the interface structures equals 10 Å. The conduction band effective mass m_e is taken to be $0.067m_0$ [19] with m_0 the free-electron mass. We have also calculated hole valence minibands of the LSSLW with the mixing of the light- and heavy-hole bands neglected, as shown in figure 3(*b*). We considered an averaged parabolic valence hole band with an effective mass $M_h = 0.3m_0$ [19]. For the same LSSLW structures described above, the first minigap of the hole valence minibands is $\Delta E_g^v(1) = 11.7$ meV, much less than that of the conduction minibands owing to the heavy-hole mass.

The effects of the periodic potential on the impurity states in the GaAs/AlAs LSSLW are not as drastic as that on the free-electron states. Although the periodic potentials cause broadenings and shifts in the peaks of the impurity density of states, from figure 2 the impurity density of states remains almost the same as that in quantum well wires with planar interfaces. The width of the donor impurity band is $\Delta E_D = 15.7$ meV for the GaAs/AlAs LSSLW with the same structures described above. We have also calculated the acceptor impurity band for the same GaAs/AlAs LSSLW structure with the averaged parabolic hole valence band approximation. The width ΔE_A of the acceptor impurity band obtained is 26.0 meV.

It is interesting to note that the periodic potential along the LSSLW direction will change the impurity $\rightleftarrows$ band optical transitions considerably, especially for the acceptor impurity $\rightarrow$ conduction band transition. Because the first minigap ($\Delta E_g^c(1) = 52.6$ meV) of the conduction band caused by the periodic potential is much larger than the width

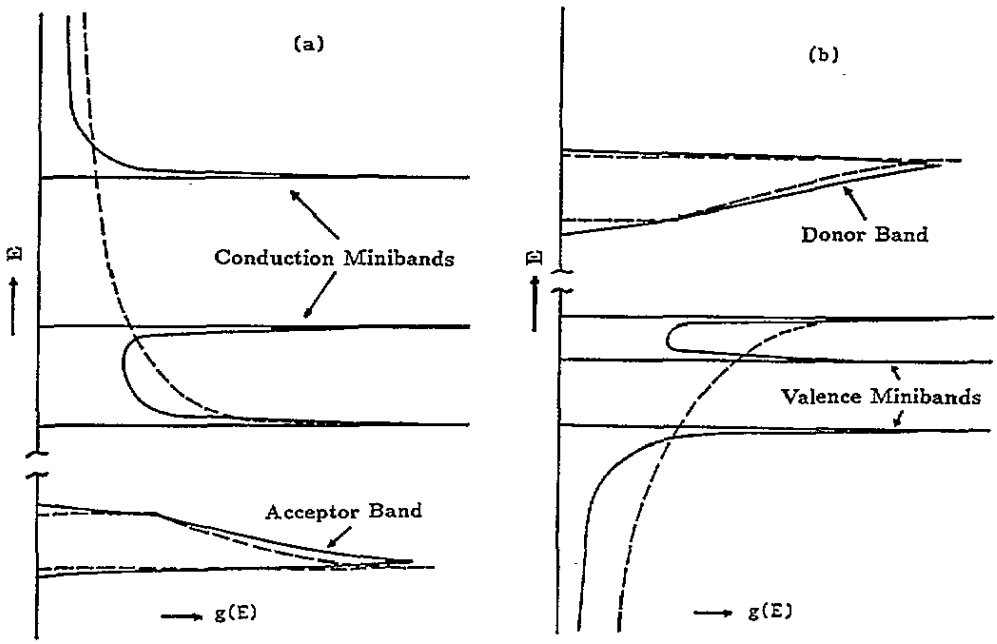

Figure 3. The distribution of the densities of states in the donor and acceptor bands and in the first two conduction and valence minibands, where the average radius R_0 of the LSSLW is 50 Å, the amplitude Δ and period L_d of the interface structures of the LSSLW are 10 Å and 100 Å, respectively. The dashed lines represent the corresponding results in the quantum wire without lateral surface structures. In order to discuss optical transitions conveniently, (*a*) the first two conduction minibands with the acceptor band and (*b*) the donor band with the first two valence minibands are plotted in the two figures separately.

($\Delta E_A = 26.0$ meV) of the acceptor impurity band, the acceptor impurity $\rightarrow$ conduction band transition becomes forbidden owing to the energy conservation law when the incident light energy lies in the region $\Delta E_A + E_{AC} \leqslant \hbar\omega \leqslant E_{Ac} + \Delta E_g^C(1)$, where E_{AC} is the energy space between the bottom edge of the first minigap of the conduction band and the top edge of the acceptor impurity band. Therefore the new peaks of the acceptor impurity $\rightarrow$ conduction band optical transition will appear because of the existence of the new peaks in the conduction electronic density of states at the energies near the edge of the minigap. For the valence band $\rightarrow$ donor impurity band optical transition, the energy-forbidden region does not exist because the first minigap ($\Delta E_g^V(1) = 11.7$ meV) of the hole valence band is smaller than the width ($\Delta E_D = 15.7$ meV) of the donor impurity band, but a new sunken structure in the valence band $\rightarrow$ donor impurity band optical transition spectrum is expected. In this work, we consider only the impurities distributing homogeneously in the LSSLW. If a realistic impurity distribution is included, the densities of impurity states in the LSSLW become more complicated [22], but the widths of the impurity band change little. Detailed results of the impurity $\rightleftarrows$ band optical transitions in the LSSLW will be given elsewhere.

Summing up, we have studied the energy miniband structures and the densities of impurity states in the LSSLW using a coordinate transformation. The results show that the EMGs and new peaks in the electronic density of states of the LSSLW will appear compared with the electronic density of states in the usual quantum well wire, but the impurity states of the LSSLW will not be greatly changed except for a small broadening of the impurity bands.

The new optical transition spectral structures are expected to appear between acceptors and *conduction minibands* in the LSSLW.

References

[1] Asada M, Miyamoto Y and Suematsu Y 1985 *Japan. J. Appl. Phys.* **24** L95
[2] Miyamoto Y, Cao M, Shingai Y, Furuya K, Suematsu Y, Ravikumar K G and Arai S 1987 *Japan. J. Appl. Phys.* **26** L225
[3] Asada M, Miyamoto Y and Suematsu Y 1986 *IEEE J. Quantum Electron.* **QE-22** 1915
[4] Suemune I and Coldren L A 1988 *IEEE J. Quantum Electron.* **QE-24** 1178
[5] Bastard G 1981 *Phys. Rev.* B **24** 4714
[6] Mailhiot C, Chang Y C and McGill T C 1982 *Phys. Rev.* B **26** 4449
[7] Stopa M and DasSarma S 1989 *Phys. Rev.* B **40** 8466
[8] Lee J and Spector H N 1984 *J. Vac. Sci. Technol.* B **2** 16
[9] Bryant G W 1984 *Phys. Rev.* B **29** 6632
[10] Brum J A 1985 *Solid State Commun.* **54** 179
[11] Bryant G W 1985 *Phys. Rev.* B **31** 7812
[12] Brown J W and Spector H N 1986 *J. Appl. Phys.* **59** 1179
[13] Osorio F A P, Degani M H and Hipolito O 1988 *Phys. Rev.* B **37** 1402
[14] Weber G, Schulz P A and Oliveira L E 1988 *Phys. Rev.* B **38** 2179
[15] Gold A and Ghazali A 1990 *Phys. Rev.* B **41** 7626
[16] Montenegro N P, Lopez-Gondar J and Oliveira L E 1991 *Phys. Rev.* B **43** 1824
[17] Chuu D S, Hsiao C M and Mei W N 1992 *Phys. Rev.* B **46** 3898
[18] Branis S V, Li G and Bajaj K K 1993 *Phys. Rev.* B **47** 1316
[19] Oliveira L E and Perez-Alvarez R 1989 *Phys. Rev.* B **40** 10460
[20] Montenegro N P and Oliveira L E 1990 *Solid State Commun.* **76** 275
[21] Weber G and Oliveira L E 1990 *Mater. Sci. Forum* **65–66** 135
[22] Latge A, Montenegro N P and Oliveira L E 1992 *Phys. Rev.* B **45** 6742
[23] Tanaka M and Sakaki H 1988 *Japan. J. Appl. Phys.* **27** L2025
[24] Tsuchiya M, Gaines J M, Yan R H, Simes R J, Holtz P O, Coldren L A and Petroff P M 1989 *Phys. Rev. Lett.* **62** 466
[25] Tanaka M and Sakaki H 1989 *Appl. Phys. Lett.* **54** 1326
[26] Sham L J 1991 *Proc. Int. Semin. on Physics of Semiconductor Interfaces and Heterostructures (Beijing, 1991)*
[27] Gerhardts R R, Weiss D and Klitzing K V 1989 *Phys. Rev. Lett.* **62** 1173
[28] Winkler R W, Kotthaus J P and Ploog K 1989 *Phys. Rev. Lett.* **62** 1177
[29] Citrin D S and Chang Y C 1991 *J. Appl. Phys.* **70** 867
[30] Cibert J, Petroff P M, Dolan G J, Pearton S J, Gossard A C and English J H 1986 *Appl. Phys. Lett.* **49** 1275
[31] Sun H 1992 *J. Phys.: Condens. Matter* **4** L213
[32] Deng Z Y, Sun H and Gu S W 1992 *J. Phys.: Condens. Matter* **4** 6549
[33] Deng Z H, Sun H and Gu S W 1992 *Phys. Lett.* **169A** 186
[34] Deng Z H, Sun H and Gu S W 1993 *J. Phys.: Condens. Matter* **5** 757